Molecular Diversity
https://doi.org/10.1007/s11030-022-10453-1

ORIGINAL ARTICLE

Exploration of 4-aminopyrrolo[2,3-*d*]pyrimidine as antitubercular agents

Omobolanle Janet Jesumoroti[1] · Richard M. Beteck[1] · Audrey Jordaan[2] · Digby F. Warner[2,3,4] · Lesetja J. Legoabe[1]

Received: 24 January 2022 / Accepted: 26 April 2022

Abstract

Tuberculosis (TB) is one of the leading causes of death worldwide. Developing new anti-TB compounds using cost-effective processes is critical to reduce TB incidence and accomplish the End TB Strategy milestone. Herein, we describe the synthesis and structure–activity relationships of a library of thirty *7H*-Pyrrolo[2,3-*d*]pyrimidine derivatives providing insights into the contributions of different aromatic, aryl and alkyl substitution at the C-4 position of the 7-deazapurine ring. The minimum inhibitory concentration (MIC) of the compounds against the green fluorescent protein (GFP) reporter strain of *Mycobacterium tuberculosis* was assayed using the standard broth microdilution method, and cell toxicity was determined using the MTT assay. Sixteen compounds displayed in vitro activity against the GFP reporter strain of *Mycobacterium tuberculosis* with MIC_{90} values of 0.488–62.5 µM. This study highlights the most potent derivative, *N-(4-phenoxy phenyl)-7H-pyrrolo[2,3-d]pyrimidin-4-amine* with a MIC_{90} value of 0.488 µM and was non-cytotoxic to the Vero cell line. Moreover, all the potent compounds from this series have a ClogP value less than 4 and molecular weight < 400; thus, likely to maintain drug-likeness during lead optimisation.

Graphical abstract

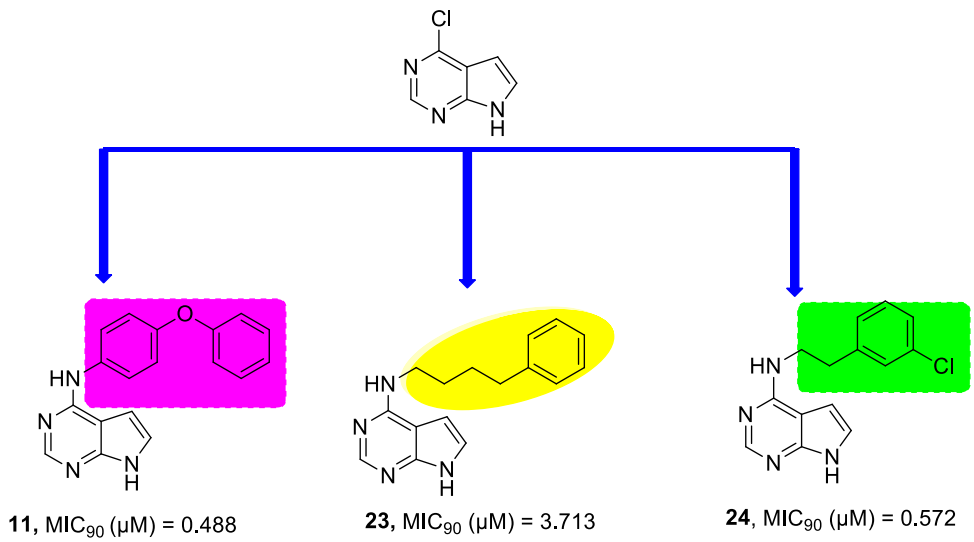

Keywords Antitubercular activity · 7*H*-pyrrolo [2,3-*d*] pyrimidines · Cytotoxicity · SAR · Tuberculosis

✉ Lesetja J. Legoabe
lesetja.legoabe@nwu.ac.za

Extended author information available on the last page of the article

Published online: 22 May 2022

Introduction

Tuberculosis (TB), an infectious disease caused by *Mycobacterium tuberculosis* (Mtb) [1], is one of the top ten causes of mortality worldwide and the second leading cause of death (after Covid-19) from a single infectious agent [2]. While the annual number of TB deaths is reducing globally, the progress has been very slow, with a cumulative drop of 14% between 2015 and 2019, which was less than half of the target of a 35% reduction between 2015 and 2020 [2]. The Covid-19 pandemic is a major concern since it has halted years of progress in providing vital TB services aimed at reducing TB burden; this has resulted in an upsurge in TB mortality. The best predictions for TB-related deaths in 2020 are: 1.3 million fatalities among HIV-negative people (up from 1.2 million in 2019) and an additional 214,000 fatalities among HIV-positive people (up from 209,000 in 2019) [3]. As a result, global TB targets are generally off-track. Thus, it is unlikely that TB will be eradicated as a global public health hazard by 2035, as the End TB Strategy anticipates [4].

One serious challenge in the treatment of tuberculosis is the emergence of multi-drug-resistant strains of *Mtb* which arises due to improper use of both traditional first-line and second-line antituberculosis drugs [5]. Globally in 2019, approximately half a million people developed rifampicin-resistant TB (RR-TB), with 78% of patients presenting with multidrug-resistant TB (MDR-TB). In 2019, about 3.3% of new TB cases and 17.7% of previously treated cases were MDR/RR-TB [2]. Therefore, to curb the menace of increasing resistance and unaffordable treatment, it is crucial to develop novel anti-TB agents based on cost-effective procedures.

To the best of our knowledge, no *7H*-pyrrolo[2,3-*d*] pyrimidine-based drug is currently in clinical use as an antituberculosis agent. Mtb has a cell envelope that is permeable to nucleosides. The uptake of many antibiotics is hampered by this envelope. The discovery of several nucleoside analogues with antitubercular action suggests that these agents are easily transported into Mtb [6, 7]. Since 7-deazupurine is a purine (nucleosides) analogue (Fig. 1), [8, 9], it might be transported across the envelope through the same transport mechanism utilised by native purines. It is likely that compounds differing in their mechanism of action from existing drugs and, as a result, active against multidrug-resistant tuberculosis strains, can be found among the *7H*-pyrrolo[2,3-*d*] pyrimidine-based compounds. Thus, in our continuous effort to develop new anti-tubercular agents, we have focused our attention on the synthesis of *7H*-pyrrolo[2,3-*d*]pyrimidine (7-deazapurine) derivatives.

7H-Pyrrolo[2,3-*d*]pyrimidine (7-deazapurine), analogous to purine, is one of the interesting classes of *N*-heterocycles that has been classified as a privileged medicinal scaffold with diverse biological activities [10, 11]. The pyrimidine ring is the building block of DNA and RNA, thus, one possible reason for the wide biological activities of pyrimidine-containing molecules [12–14]. Pyrrolo[2,3-*d*]pyrimidine nucleus is often encountered in some approved drugs, clinical candidates, and functional material. Drugs currently in the market that possess pyrrolo[2,3-*d*]pyrimidine skeleton include anti-cancer drugs such as ruxolitinib, tofacitinib, and baricitinib [10]. Compounds with pyrrolo[2,3-*d*]pyrimidine moiety have broad biological applications such as antibacterial, antifungal [15, 16], adenosine A_1 and A_3 receptor modulator [17], protein-kinase B inhibitor [18], anti-inflammatory [19], anti-cancer [20, 21], anti-folate [22], antiviral [23, 24], and anti-mycobacterial activities [25–27]. Additionally, some naturally occurring antibiotics such as tubercidin, toyocamycin, sangivamycin (Fig. 1) have pyrrolo[2,3-*d*]pyrimidine moiety and exhibited significant activity against Mtb,

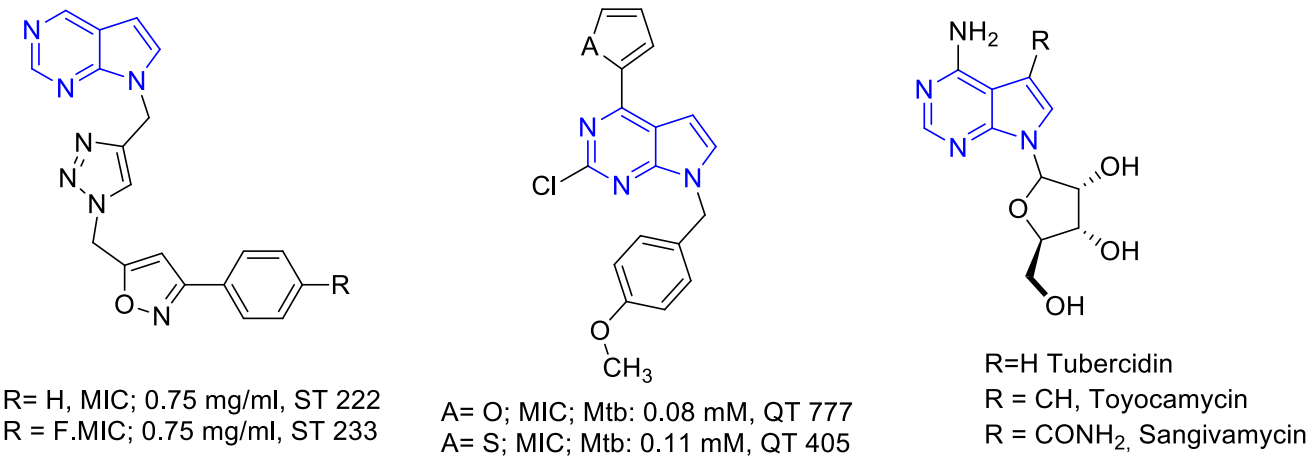

Fig. 1 Structures of 7-deazupurine-based antitubercular agents and structurally related scaffolds

Candida albicans and *Cryptococcus neoformans* [28–32]. In recent years, among the *7H*-pyrrolo[2,3-*d*]pyrimidine derivatives, the search for synthesized compounds possessing anti-tubercular activity (Fig. 1) has been less explored with only a few reports [32, 33]. More specifically, a previous report identified 7-deaza purine analogs (QTT 777 and QTT 405) (Fig. 1) modified in the five-membered ring to displayed excellent anti-tubercular activity against the H37Rv strain of Mtb in vitro, with MIC values between 0.08 and 0.35 µM. These values are comparable or better than the reference drug (Rifampicin 0.09 µM) [33]. Thus, *7H*-pyrrolo[2,3-*d*]pyrimidine nucleus can be exploited further in search of affordable new agents for the treatment of TB.

In this work, we report on acid-catalysed chemo-selective C-4 substitution of *7H*-pyrrolo[2,3-*d*]pyrimidine (7-deazapurine) ring with various amines and the antitubercular activity of the resultant compounds. Scinfinder and Pubmed were used to determine the novelty of each compound's structure. Compounds **1**, **4**, **6**, **7**, **8**, **9**, **10**, **11**, and **16** had already been reported [34]. The remaining 21 compounds (compounds **2**,**3**, **12–15** and **17–31** have no previous references; hence, they were classified as novel. Despite this, none of the compounds had been previously investigated as anti-tubercular agent.

Result and discussion

Chemistry

The synthesis of compounds **1–31** was achieved in a simple and straightforward method by treating commercially available 4-chloro-7*H*-pyrrolo[2,3-*d*]pyrimidine with different aromatic, aliphatic, cyclic, cyclo aliphatic, and aryl aliphatic amines in the presence of a catalytic amount of HCl (Fig. 2). Target compounds were obtained in 16–94% yields. In general, in the ^{1}H NMR spectra, the broad singlet signals appearing at *ca* 11.47 ppm of all the compounds are attributed to the presence of –NH– moiety in the pyrrolyl ring. The singlet appearing in the range 8.63–8.67 ppm is attributed to H-2, and the doublet or doublet of doublets peak in the range of δ 7.31–6.51 ppm are assigned to H-6 or H-5. The change from doublet of doublets to a doublet of H-5 and H-6 is attributed to the replacement of hydrogen at N-7 by deuterium. The assignments for H-5 and H-6 are consistent with the literature review[35]. The NMR spectra are consistent with those reported in the literature [34]. The broad singlet signal or triplet at 9.84–7.84 ppm corresponds to –NH– at position C-4 (for Ar–N<u>H</u> and –N<u>H</u>CH$_2$, respectively), and this suggests the successful nucleophilic substitution of the Cl atom in 4-chloro-7*H*-pyrrolo[2,3-*d*]pyrimidine. In the ^{13}C NMR spectra, resonances for all the carbons are observed. Typically, the signal appearing at *ca* 55–56 ppm of all the compounds is indicative of the methylene carbon next to *7H*-pyrrolo[2,3-*d*]pyrimidine nitrogen. The exact mass for all target compounds is confirmed using high-resolution mass spectrometry (HRMS).

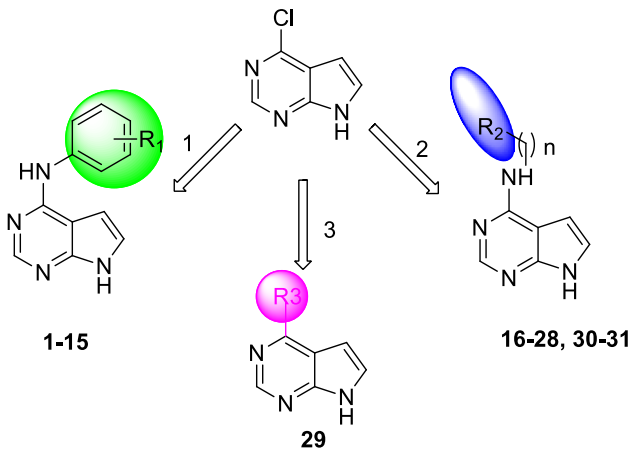

Fig. 2 Design strategy for *7H*-pyrrolo[2,3-*d*]pyrimidine analogs

Biological evaluation

In vitro antitubercular screening

In vitro antitubercular activity of the target compounds **1–31** was investigated against the green fluorescent protein (GFP) reporter strain of Mtb cultured for 14 days using Middlebrook 7H9 medium supplemented with glucose, casitone, and tyloxpol. The standard, rifampicin, a first-line antitubercular agent, was used as a reference. All the target compounds were tested in a concentration range of 0.0002–10 mM, and a dose–response curve was plotted for each compound. The minimum inhibitory concentration (MIC) was defined as the least compound concentration required to inhibit 90% (MIC_{90}) of bacteria growth, and the MIC values are given in Table 1. Sixteen (16) out of the thirty-one (31) compounds evaluated were active against Mtb, exhibiting activity in the range 0.488–62.5 µM. Five compounds (**10**, **11**, **15**, **23,** and **24**) showed excellent potency against Mtb with a MIC value of < 4 µM.

Structural activity relationship (SAR) For the subseries containing compounds **1**–**15**, where R represents a phenyl ring, antitubercular activity generally vary with the position of halogen on the phenyl ring. The SAR in Table 1 revealed that the 3-halo (meta; C-3) (compounds **6,9**) and 2-halo (ortho; C-2) substituted phenyl derivatives (compound **7**) showed slightly improved anti-tubercular activity than the 4-halo (para; C-4) substituted derivatives (compound **2** and **8**). This suggests that *meta* and *ortho*-substituted phenyl

compounds can easily penetrate the bacterial cell and have suitable binding interactions with their target.

The introduction of different halogen atoms on the phenyl ring caused different effects on the antitubercular activity against the GFP reporter strain of Mtb. The presence of a bromine atom seems to generally favour antitubercular activity over other halogens such as chlorine and fluorine. Replacing the chlorine atom in compound **6** ($MIC_{90:}$ 31.25 μM) with a bromine atom to afford compound **9** ($MIC_{90:}$ 15.625 μM) led to a twofold increase in antitubercular activity. This trend is also observed when comparing compound **8** ($MIC_{90:}$ 125 μM) bearing *para* chlorine against its *para* bromine analogue, compound **10** ($MIC_{90:}$ 3.9 μM), with the bromine bearing analogue still showing superior antitubercular activity. Moreover, compound **2** ($MIC_{90:}$ 125 μM), the fluorine analogue of compound **10** is also inactive. This suggests that achieving good antitubercular potency with 7-deazupurine requires a combination of both increased size and polarizability of the substituent on the phenyl ring.

The presence of fluorine atom on the phenyl ring (compound **2**,**3;** $MIC_{90:}$ 125 μM) generally resulted in the loss of antitubercular activity when compared with unsubstituted phenyl derivative, compound **1** ($MIC_{90:}$ 62,5 μM). This might be due to the lower electron density of the fluoro-substituted phenyl ring caused by the electron-withdrawing effect of fluorine, which may reduce the binding affinity between the compound and the target, thus decreasing its antitubercular activity. The effect of the fluorine atom is further tested by comparing compound **5** ($MIC_{90:}$ 125 μM) against its defluoronated analogue, compound **6** ($MIC_{90:}$ 31.25 μM). This again suggests that the presence of a fluorine atom is detrimental to antitubercular activity.

Other electron-withdrawing groups (NO_2, compounds **13**; CF_3, compound **4**) or a combination of electron-donating and electron-withdrawing (OCH_3 & NO_2, compound **14**) groups were tested and found to have a different effect on antitubercular activity compared to fluorine. Compounds **4** and **13** ($MIC_{90:}$ 62.5 μM) exhibited equal antitubercular activity compared to their unsubstituted analogue **1** and better than their fluorinated counterparts (compound **2** and **3**).

An increase in the size of substituent attached to the phenyl ring was also investigated using compounds **11** and **15**. Compounds bearing 4-morpholino or 4-phenoxyl moiety on the phenyl ring as seen in compounds **15** and **11**, respectively, exhibited relatively good to excellent antitubercular activity compared to compound **1**, bearing an unsubstituted phenyl ring. Compound **11** with a 4-phenoxy substituent on the phenyl ring was the most potent with MIC_{90}: 0.488 μM and compound **15** with a 4-morpholino substituent on the phenyl ring exhibited significant antitubercular activity MIC_{90}: 3.906 μM. This shows that increased ring size of substituents on the aniline moiety at position 4 of 7-deazupurine plays an important role in antitubercular activity (Fig. 2).

In subseries **16–24**, the effect of methylene spacers between the phenyl and the amino moieties and/or phenyl substitution was investigated. In general, antitubercular activity seems to vary with the methylene chain length between the phenyl ring and the secondary amine at C-4 of 7-deazupurine. The results (Table 1) showed that compound **16** (MIC_{90}: 62.5 μM) bearing a benzylamine (one methylene spacer) exhibited comparable activity with compound **1** (MIC_{90}: 62.5 μM) bearing aniline moiety (no methylene spacer). Compound **21** (MIC_{90}: 31.25 μM) bearing phenylethylamine (two methylene spacers) displayed improved activity compared to **16**, and compound **22** (MIC_{90}: 14.452 μM) bearing three methylene spacers showed better activity compared to **21**. Compound **23** (MIC_{90}: 3.713 μM) with four methylene spacers is the most active compound in this subseries. The antitubercular activity of compound **16** (MIC_{90}: 62.5 μM), **21** (MIC_{90}: 31.25 μM), **22** (MIC_{90}: 14.452 μM), and **23** (MIC_{90}: 3.713 μM) increases as the methylene spacers increase from 2 to 4, demonstrating that flexibility of C-4 substituents is important for antitubercular activity. Besides the effect of methylene spacers on antitubercular activity, the influence of phenyl substituents in the subseries **16**–**24** was also investigated. Comparing compound **21** against its congener, compound **24** (MIC_{90}: 0.572 μM), bearing *meta* chlorophenylethylamine again confirms that meta substituted phenyl moieties enhance antitubercular activity. It is interesting to note that compound **24** (MIC_{90}: 0.572 μM), wherein R is 2-(3-Chlorophenyl)ethyl, displayed excellent activity compared to compound **21** (MIC_{90}: 31.25 μM) wherein R is phenylethyl. This shows that both the methylene spacers and the position of chloro substituents on the aryl moiety are crucial for antitubercular activity (Fig. 3)

In addition, considering the effect of substituent with alkyl chains linked to the amino group at position 4 of the core 7-deazupurine), the SAR study revealed that the introduction of the aliphatic chain was detrimental to such activity. Thus, the replacement of the phenyl group at the terminal end of the alkyl chain with hydrophilic groups such as hydroxyl, or substitution by methyl markedly resulted in the loss of activity. This is evident in compound **25**, **26**, **27**, **28** wherein R is *N*-isopentyl, 2-((2-aminoethyl)amino) ethanol, 3-isopropoxypropyl, 3-morpholinopropyl, respectively, and, all exhibited no significant antitubercular activity ($MIC_{90} > 125$ μM) as compared to compound **22** ((MIC_{90}: 14.452 μM). These data indicate that the phenyl group at the terminal end of the alkyl chain attached to NH on C-4 of 7-deazapurines is a prerequisite for antitubercular activity.

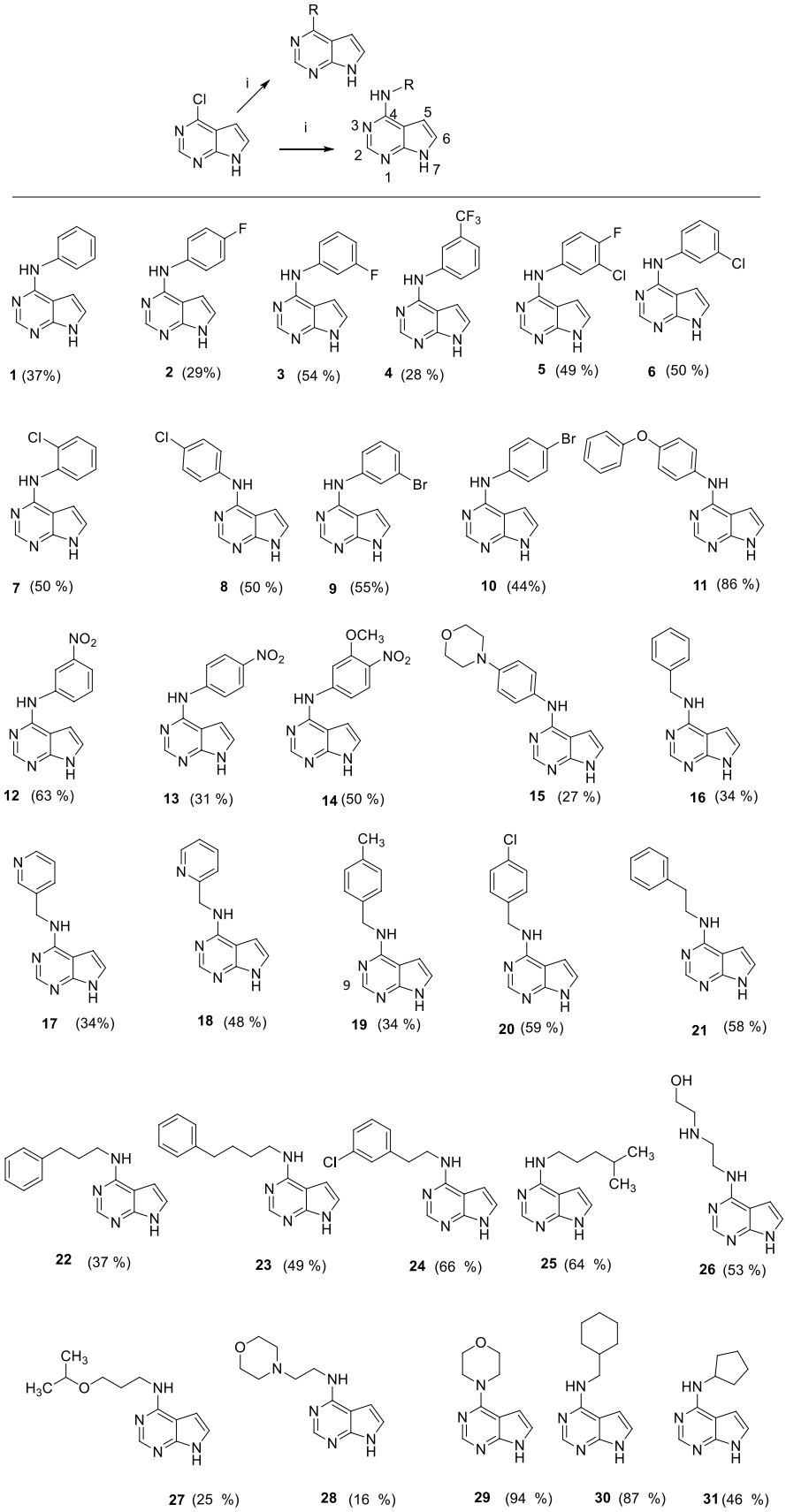

Fig. 3 Structures and the percentage yields of the synthesised compounds from this study

Table 1 ClogP and MIC_{90} values of target compounds compared against rifampicin (standard drug)

Compound	ClogP	MIC_{90}(μM)
1	2.24	62.5
2	2.56	> 125
3	2.55	> 125
4	2.14	62.5
5	1.82	125
6	2.77	31.25
7	2.80	31.25
8	2.78	125
9	2.86	15.52
10	2.88	**3.90**
11	3.43	**0.48**
12	1.64	> 125
13	1.66	62.5
14	1.47	> 125
15	1.56	**3.90**
16	2.23	62.5
17	1.50	30.44
18	1.47	125
19	2.55	> 125
20	2.77	125
21	2.51	31.25
22	2.83	14.45
23	3.16	**3.71**
24	2.57	**0.57**
25	2.20	125
26	0.33	125
27	1.92	125
28	1.14	125
29	0.96	30.04
30	2.63	15.62
31	2.01	125
RF	–	**0.01**

[a]Clog *P* values calculated with the Swiss ADME web tool (http://www.swissadme.ch/)

[b]MIC_{90} = determined in vitro against GFP *Mtb* strain, *RF* rifampicin

Cytotoxicity

The in vitro cytotoxic properties of the most active compound (**11**) were evaluated at different concentrations (1, 5, and 10 μM) against two cell lines: BJ-5ta (hTERT immortalized Human skin fibroblasts) and Vero cell lines. Compound **11** showed a concentration-dependent reduction in the viability of the BJ-5ta cell line during a 48 h exposure. Low concentrations (1 μM) seem to induce cell growth, with a viability of 115% which is more than that of the untreated control (100%). At 10 μM, this compound is weakly cytotoxic towards the BJ-5ta cells, reducing cell viability to 70% (Fig. 4) [36]. However, this compound does not appear to be toxic against the Vero cell line with no cell viability reduction observed at the highest concentration tested (Fig. 5). The results suggested that compound **11** possessed little overt cytotoxicity risk against the human cell lines tested.

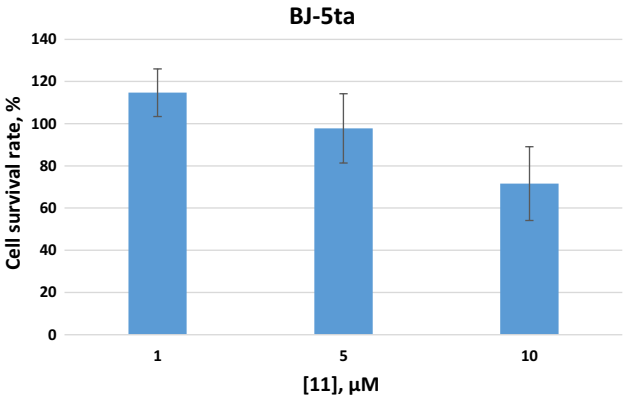

Fig. 4 Cell survival following treatment of BJ-5ta cells for 48 h with compound **11** in comparisons with the untreated control, as determined with the MTT assay (error bars = standard deviation, $n = 3$)

In Silico drug likeliness Studies

Specific physicochemical properties are required for antibacterial drugs which distinguished them from other drugs. The unique design of the bacterial cell wall necessitates antibacterial agents to have specific properties in order to cross the cell wall. Such physicochemical properties include lower higher molecular weights and increased total polar surface area when compared to other drugs classes [37]. The drug-like properties (including Lipinski rule of five, GI absorption, and CYP2C19 inhibition) of the most

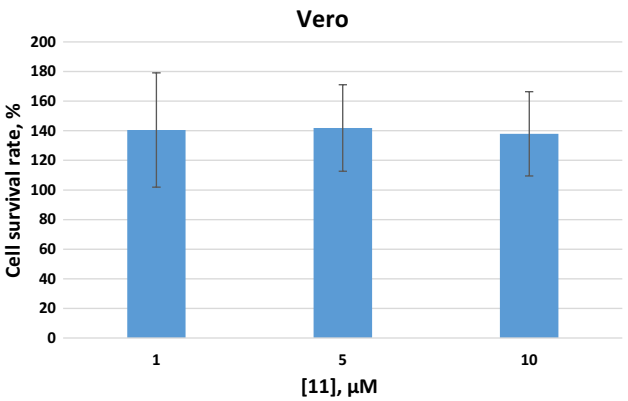

Fig. 5 Cell survival following treatment of Vero cells for 48 h with compound **11** in comparisons with the untreated control, as determined with the MTT assay using (error bars = standard deviation, $n = 3$)

Table 2 Computed properties of the selected active compounds using SWISS ADME

	Compound **11**	Compound **23**	Compound **24**
MW g/mol	302.33	266.34	272.73
Log S[a] *(ESOL)*[b]	−4.69	−3.95	−4.09
Log S[1] *(Ali)*[c]	−5.09	−4.46	−4.37
H donor	2	2	2
H acceptor	3	2	2
Lipinski #violation	0	0	0
[d]TPSA (Å^2)	62.83	53.60	53.60
No of rotatable bonds	4	6	4
GI absorption	High	High	High
CYP2C19 Inhibitor	Yes	Yes	Yes
[e]Drug Likeness	Yes	Yes	Yes

[a]Predicted aqueous solubility, where log S is the logarithm of the amount of compound (in moles) able to dissolve in a litre of water

[b]ESOL, predicted aqueous solubility, calculated using a topological method[38]

[c]Estimated aqueous solubility using a topological method [39] with log S scale: insoluble < −10 < poorly < −6 < moderately < −4 < soluble < −2 very soluble < 0 highly soluble

[d]TPSA, topological polar surface area, polarity: TPSA between ≤ 140 Å^2[40]

[e]Calculated with reference to Lipinski's rule of five: MW ≤ 500 g/mol; log $P \leq 5$; HBD ≤ 5; HBA ≤ 10; no more than one violation allowed [41]

potent compounds **11**, **23**, and **24** were evaluated in silico (Table 2) using the SwissADME web tool (http://www.swissadme.ch/).

The active compounds from this study have a molecular weight of less than 400 Da and calculated lipophilicity (ClogP) of less than 4, which make them ideal compounds for hit to lead optimization. Other drug-like properties including oral bioactivity and solubility were predicted using the SwissADME web tool. The predicted solubility of compounds **11**, **23** and **24** ranges from −3.95 to −5.09; thus, these compounds are predicted to be moderately water-soluble. The flexibility defined as the number of rotatable bonds of all the active compounds are less than 9. Also, the polarity describes as the total polar surface area (tPSA) for the active compounds is less than 140 Å^2 (or a total number of both H-bond donors and acceptors is less than 10). Thus, these compounds are predicted to have good oral bioavailability The predicted drug-likeness properties of all the active compounds identified in this study showed that they do not violate any of the parameters of the Lipinski's rule of five [41]. All the active compounds from this study are predicted to possess good passive human gastrointestinal absorption and blood–brain barrier permeation.

Conclusion

In conclusion, we successfully synthesized a series of thirty derivatives of 7*H*-pyrrolo[2,3-*d*]pyrimidine with good antitubercular properties against the GFP reporter strain of Mtb. The most active compound in the series is **11** ($MIC_{90} = 0.488$), which was evaluated for cytotoxicity potentials against Human skin fibroblasts hTERT and Vero cell lines. The compound displays weak cytotoxicity against the BJ-5ta cell line but possesses no potential cytotoxicity risk against Vero cell lines. Also, the SAR study suggested that site substituted on the phenyl ring and methylene spacers between the phenyl and amine moieties at C-4 of 7-deazupurine influence antitubercular activity. All the potent compounds in this series have molecular weights less than 400 Da and ClogP less than 4, which suggests they are likely to maintain drug-likeness during lead optimisation. The results from this study provide evidence that compounds based on 7*H*-pyrrolo[2,3-*d*]pyrimidine could be further explored for the discovery of new compounds against TB.

Experimental

Chemistry

The chemicals and solvents used in this study were purchased from various chemical vendors: Sigma-Aldrich (Pty) Ltd. (Johannesburg, South Africa), Merck (Pty) Ltd. (Johannesburg, South Africa) and were used without purification. The progress of the reactions was monitored by thin-layer chromatography (TLC) using Merck $60F_{254}$ silica gel plates (Merck, Johannesburg, South Africa) supported on aluminium, and the plates were visualized under ultraviolet (UV254 and 366 nm) light or stained with iodine vapour. ^{1}H and ^{13}C NMR spectra were recorded on Bruker Biospin 600 MHz spectrometer, and the chemical shifts are given in values referenced to deuterated DMSO-d_6 and are reported in parts per million (ppm). Chemical shifts for deuterated DMSO-d_6 appear at 2.5 ppm for ^{1}H and 39.5 ppm for ^{13}C NMR spectra. Proton coupling patterns are abbreviated as follows: s (singlet), d (doublet), dd (doublet of doublet), t (triplet), q (quartet), and m (multiplet). Coupling constants (J) are reported in Hz. NMR data were analysed using MestReNova Software, version 5.3.2–4936. Melting points (mp) were established with a Büchi melting point B-545 instrument and were uncorrected. The High-resolution mass spectra (HRMS) were recorded using a Bruker micrOTOF-Q II mass spectrometer using atmospheric pressure chemical ionization (APCI) in positive ion mode.

General Procedure for the synthesis of compound 1–15

The 7*H*-pyrrolo[2,3-*d*]pyrimidine derivatives **1**–**15** were synthesized via acid-mediated nucleophilic substitution reaction of 4-chloro-7*H*-pyrrolo[2,3-*d*]pyrimidine (200 mg, 1.3 mmol) with the appropriate amines. The 4-chloro-7*H*-pyrrolo[2,3-*d*]pyrimidine (200 mg, 1.3 mmol) and appropriate anilines (3 equiv) were dissolved in 5 ml of isopropanol, and 3-drops of conc HCl were added. The mixtures were refluxed for 12 h. After this time, the mixtures were allowed to cool to room temperature and then, concentrated on a rotary evaporator. Water (10 ml) and 1 mL of aqueous NH_4OH were added, followed by extraction with $CHCl_3$ (12 ml × 3). The organic layers were dried over Na_2SO_4, filtered, and concentrated under reduced pressure to afford the crude mixtures. The crude solids were recrystallized from a suitable solvent (e.g. methanol) to afford the target compounds in yields of 27–86% yield.

General Procedure for the synthesis of compound 16–31

The 7*H*-pyrrolo[2,3-*d*]pyrimidine derivatives **16**–**31** were synthesized via acid-mediated nucleophilic substitution reaction of 4-chloro-7*H*-pyrrolo[2,3-*d*]pyrimidine (200 mg, 1.3 mmol) with the appropriate amines (3 equiv). The 4-chloro-7*H*-pyrrolo[2,3-*d*]pyrimidine (200 mg, 1.3 mmol) and the appropriate amines were dissolved in 5 ml of isopropanol, and 3-drops of conc HCl were added. The mixtures were refluxed for 12–48 h, allowed to reach room temperature, and water (10 ml) was added to precipitate out the products. The crude products were filtered, washed with water, and air-dried overnight. Recrystallization from suitable solvents (e.g. methanol) afforded the target compounds in yields of 16–94%.

N-phenyl-7H-pyrrolo[2,3-d]pyrimidin-4-amine **(1).** White powder, yield 37%, mp 241 °C. ^{1}H NMR (600 MHz, DMSO-d_6) δ 11.74 (br s, 1H, NH, H-7), 9.29 (s, 1H, NH), 8.27 (s, 1H, H-2), 7.89 (d, J = 7.7 Hz, 2H, Ar–H), 7.33 (t, J = 7.9 Hz, 2H, Ar–H), 7.23 (dd, J = 3.5, 1.7 Hz, 1H, H-6), 7.01 (t, 1H, J = 7.3, Ar–H), 6.79 (d, J = 2.9 Hz, 1H, H-5).^{13}C NMR (151 MHz, DMSO-d_6) δ 153.6, 150.9, 150.8, 140.4, 128.5, 122.1, 121.9, 120.3, 103.7, 98.8. HRMS (APCI) *m/z*: calcd for $C_{12}H_{11}N_4$ $[M+H]^+$: 211.0978, found: 211.0981.

N-(4-fluorophenyl)-7H-pyrrolo[2,3-d]pyrimidin-4-amine **(2).** Grey powder, yield 29%, mp 253 °C. ^{1}H NMR (600 MHz, DMSO-d_6) δ 11.74 (br s, 1H, NH, H-7), 9.32 (s, 1H, NH), 8.25 (s, 1H, H-2), 7.88 (dd, J = 9.1, 5.0 Hz, 2H, Ar–H), 7.23 (d, J = 3.4 Hz, 1H, H-6), 7.17 (t, J = 8.9 Hz, 2H, Ar–H), 6.75 (d, J = 3.4 Hz, 1H, H-5). ^{13}C NMR (151 MHz, DMSO-d_6) δ 158.5 ($^1J_{CF}$ = 238.6 Hz), 153.5, 150.8, 150.8, 136.7 ($^4J_{CF}$ = 1.5 Hz), 122.2. 121.9 ($^3J_{CF}$ = 7.6 Hz), 114.8 ($^2J_{CF}$ = 22.7 Hz), 103.5, 98.7. HRMS (APCI) *m/z*: calcd for $C_{12}H_{10}FN_4$ $[M+H]^+$: 229.0884, found 229.0887.

N-(3-fluorophenyl)-7H-pyrrolo[2,3-d]pyrimidin-4-amine **(3).** White powder, yield 54%, mp 234 °C. ^{1}H NMR (600 MHz, DMSO-d_6) δ 11.83 (brs, 1H, NH, H-7), 9.49 (s, 1H, NH), 8.34 (s, 1H, H-2), 8.05 (dd, J = 12.5, 5.9 Hz, 1H, Ar–H), 7.62 (t, J = 7.2 Hz, 1H. Ar–H), 7.42–7.23 (m, 2H, Ar–H, H-6), 6.88–6.73 (m, 2H, H-5, Ar–H).^{13}C NMR (151 MHz, DMSO-d_6) δ 162.2 ($^1J_{CF}$ = 240.1 Hz) 153.2, 150.9, 150.6, 142.4 ($^3J_{CF}$ = 10.6 Hz), 129.9 ($^4J_{CF}$ = 9.06 Hz) 122.6, 115.5, 108.0 ($^2J_{CF}$ = 21.1 Hz),106.5 ($^2J_{CF}$ = 27.2 Hz), 103.9, 98.7. HRMS (APCI) *m/z*: calcd for $C_{12}H_{10}FN_4$ $[M+H]^+$: 229.0884, found: 229.0883.

N-(3-(trifluoromethyl)phenyl)-7,7a-dihydro-1H-pyrrolo[2,3-d]pyrimidin-4-amine **(4).** White powder, yield 28%, mp 232 °C. ^{1}H NMR (600 MHz, DMSO-d_6) δ 11.86 (brs, 1H, NH, 7-H), 9.62 (s, 1H, NH), 8.40 (s, 1H, H-2), 8.30 (s, 1H, Ar–H), 8.24 (dd, J = 8.4, 2.2 Hz, 1H, Ar–H), 7.57 (t, J = 8.0 Hz, 1H, Ar–H), 7.33 (dd, J = 7.5, 1.6 Hz, 1H, Ar–H), 7.30 (d, J = 3.5 Hz, 1H, H-6), 6.83 (d, J = 3.4 Hz, 1H, H-5). ^{13}C NMR (151 MHz, DMSO-d_6) δ 153.1, 151.0, 150.6, 141.4, 129.5 (^{2}J$_{CF}$ = 32.8 Hz), 124.4 ($^1J_{CF}$ = 273.3 Hz), 129.7, 123.2, 122.8, 117.9 ($^4J_{CF}$ = 4.4 Hz),115.7 ($^3J_{CF}$ = 4.5 Hz), 103.9, 98.6. HRMS (APCI) *m/z*: calcd for $C_{13}H_{10}F_3N_4$ $[M+H]^+$: 279.0852, found: 279.0861.

N-(3-chloro-4-fluorophenyl)-7H-pyrrolo[2,3-d]pyrimidin-4-amine **(5).** Grey powder, yield 49%, mp > 400 °C. ^{1}H NMR (600 MHz, DMSO-d_6) δ 11.78 (br s, 1H, NH, H-7), 9.42 (s, 1H, NH), 8.32 (s, 1H, H-2), 8.29 (dd, J = 6.9, 2.7 Hz, 1H, Ar–H), 7.81-7.79 (m, 1H, Ar–H), 7.37 (t, J = 9.1 Hz, 1H, Ar–H), 7.26 (dd, J = 3.4, 2.0 Hz, 1H, H-6), 6.77 (dd, J = 3.5, 1.5 Hz, 1H, H-5).^{13}C NMR (151 MHz, DMSO-d_6) δ 153.1, 152.2 ($^1J_{CF}$ = 237.1 Hz),150.9, 150.5, 137.8 ($^4J_{CF}$ = 3.0 Hz),122.5, 121.0, 119.9 ($^3J_{CF}$ = 7.6 Hz), 118.7 ($^2J_{CF}$ = 18.2 Hz), 116.5 (^{2}J$_{CF}$ = 21.1 Hz), 103.7, 98.5. HRMS (APCI) *m/z*: calcd for $C_{12}H_9FClN_4$ $[M+H]^+$: 263.0494, found: 263.0494.

N-(3-chlorophenyl)-7H-pyrrolo[2,3-d]pyrimidin-4-amine **(6).** White powder, yield 50%, mp 227 °C. ^{1}H NMR (600 MHz, DMSO-d_6) δ 11.82 (br s, 1H, NH, 7-H), 9.49 (s, 1H, NH), 8.34 (s, 1H, H-2), 8.21 (s, 1H, Ar–H), 7.81 (dd, J = 8.2, 2.1 Hz, 1H, Ar–H), 7.35 (t, J = 8.1 Hz, 1H, Ar–H), 7.28 (d, J = 3.5 Hz, 1H, Ar–H), 7.04 (dd, J = 7.8, 2.2 Hz, 1H, H-6), 6.82 (d, J = 3.4 Hz, 1H, H-5). ^{13}C NMR (151 MHz, DMSO-d_6) δ 153.2, 151.0, 150.7, 142.1, 132.9, 130.2, 122.7, 121.4, 119.2, 118.2, 104.0, 98.8. HRMS (APCI) *m/z*: calcd for $C_{12}H_{10}Cl$ N_4 $[M+H]^+$: 245.0589, found: 245.0589.

N-(2-chlorophenyl)-7H-pyrrolo[2,3-d]pyrimidin-4-amine **(7).** White powder, yield 50%, mp: 219 °C. ^{1}H NMR (600 MHz, DMSO-d_6) δ 11.83 (br s, 1H, NH, H-7), 9.48 (s, 1H, N–H), 8.34 (s, 1H, H-2), 8.22 (t, J = 2.1 Hz, 1H, Ar–H), 7.81 (dd, J = 8.2, 2.1 Hz, 1H, Ar–H), 7.35 (t, J = 8.1 Hz,

1H, Ar–H), 7.27 (d, $J = 3.5$ Hz, 1H, Ar–H), 7.04(dd, $J = 7.9$, 2.1 Hz, 1H, H-6), 6.83 (d, $J = 3.4$ Hz, 1H, H-5). ^{13}C NMR (151 MHz, DMSO-d_6) δ 153.1, 150.9, 150.6, 142.1, 132.9, 130.1, 122.6, 121.3, 119.1, 118.1, 103.9, 98.7. HRMS (APCI) *m/z*: calcd for $C_{12}H_{10}ClN_4$ $[M+H]^+$: 245.0589, found: 245.0595.

N-(4-chlorophenyl)-7H-pyrrolo[2,3-d]pyrimidin-4-amine **(8).** White powder, yield 50%, mp 227 °C. ^{1}H NMR (600 MHz, DMSO-d_6) δ 11.80 (br s, 1H, NH, H-7), 9.42 (s, 1H, NH), 8.30 (s, 1H, H-2), 7.96 (d, $J = 8.9$ Hz, 2H, Ar–H), 7.38 (d, $J = 8.9$ Hz, 2H, Ar–H), 7.26 (dd, $J = 3.5$, 2.1 Hz, 1H, H-6), 6.80 (dd, $J = 3.5$, 1.7 Hz, 1H, H-5). ^{13}C NMR (151 MHz, DMSO-d_6) δ 153.2, 150.9, 150.6, 139.5, 128.3, 125.4, 122.4, 121.5, 103.8, 98.7. HRMS (APCI) *m/z*: calcd for $C_{12}H_{10}ClN_4$ $[M+H]^+$: 245.0589, found: 245.0576.

N-(3-bromophenyl)-7H-pyrrolo[2,3-d]pyrimidin-4-amine **(9).** White powder, yield 55%, mp: 239 °C. ^{1}H NMR (600 MHz, DMSO-d_6) δ 11.82 (br s, 1H, NH), 9.45 (s, 1H, NH, 8.33 (s, 1H, H-2), 8.32 (d, $J = 2.0$ Hz, 1H, Ar–H), 7.94–7.83 (m, 1H, Ar–H), 7.31–7.26 (m, 2H, Ar–H), 7.17 (d, $J = 8.0$ Hz, 1H, H-6), 6.81 (dd, $J = 3.5$, 1.8 Hz, 1H, H-5) ^{13}C NMR (151 MHz, DMSO-d_6) δ 153.2, 150.9, 150.6, 142.3, 130.5, 124.3, 122.7, 121.9, 121.4, 118.6, 103.9, 98.7. HRMS (APCI) *m/z*: calcd for $C_{12}H_{10}BrN_4$ $[M+H]^+$: 289.0883, found: 289.0059.

N-(4-bromophenyl)-7H-pyrrolo[2,3-d]pyrimidin-4-amine **(10).** White powder, yield 44%, mp: 2392 °C. ^{1}H NMR (600 MHz, DMSO-d_6) δ 11.79 (br s, 1H. NH, H-7), 9.45 (s, 1H, NH), 8.29 (s, 1H, H-2), 7.91 (d, $J = 8.6$ Hz, 2H, Ar–H), 7.50 (d, $J = 8.6$ Hz, 2H, Ar–H), 7.25 (d, $J = 5.7$ Hz, 1H, H-6), 6.81 (dd, $J = 3.4$, 1.9 Hz, 1H, H-5). ^{13}C NMR (151 MHz, DMSO-d_6) δ 153.2, 150.9, 150.7, 139.9, 131.3, 122.5, 121.94, 113.4, 103.9, 98.8. HRMS (ESI+) *m/z*: calcd for $C_{12}H_{10}BrN_4$ $[M+H]^+$: 289.0083, found: 289.0053.

N-(4-phenoxyphenyl)-7H-pyrrolo[2,3-d]pyrimidin-4-amine **(11).** Brown powder, yield 86%, mp 249 °C. ^{1}H NMR (600 MHz, DMSO-d_6) δ 11.74 (s, 1H, NH, H-7), 9.32 (s, 1H, NH), 8.25 (s, 1H, H-2), 7.89 (d, $J = 8.9$ Hz, 2H, Ar–H), 7.37 (t, $J = 8.0$ Hz, 2H, Ar–H), 7.28–7.19 (m, 1H, Ar–H), 7.10 (d, $J = 7.4$ Hz, 1H, Ar–H), 7.11–7.00 (m, 2H, Ar–H), 6.99 (d, $J = 7.8$ Hz, 2H, H-6), 6.76 (d, $J = 3.4$ Hz, 1H, H-5). ^{13}C NMR (151 MHz, DMSO-d_6) δ 157.7, 153.5, 150.8, 150.8, 136.4, 129.9, 122.8, 122.1, 121.9, 119.4, 117.6, 103.5, 98.7. HRMS (APCI) *m/z*: calcd for $C_{18}H_{15}N_4O$ $[M+H]^+$: 303.1240, found:303.1232.

N-(3-nitrophenyl)-7H-pyrrolo[2,3-d]pyrimidin-4-amine **(12).** Yellow powder, yield 63%, mp 359 °C. ^{1}H NMR (600 MHz, DMSO-d_6) δ 11.86 (brs, 1H, NH, H-7), 9.74 (s, 1H, NH), 8.97 (t, $J = 2.2$ Hz, 1H, Ar–H),), 8.38 (s, 1H, H-2), 8.37 (dd, $J = 2.3$, 0.9 Hz, 1H, Ar–H),), 7.84 (dd, $J = 7.8$, 1.9 Hz, 1H, Ar–H),), 7.62 (t, $J = 8.2$ Hz, 1H, Ar–H), 7.31 (d, $J = 3.5$ Hz, 1H, H-6), 6.84 (d, $J = 3.4$ Hz, 1H, H-5). ^{13}C NMR (151 MHz, DMSO-d_6) δ 152.9, 151.0, 150.4, 147.9, 141.8, 129.7, 125.4, 122.9, 115.9, 113.5, 104.0, 98.5. HRMS (APCI) *m/z*: calcd for $C_{12}H_{10}N_5O_2$ $[M+H]^+$: 256.0829, found 256.0813.

N-(3-nitrophenyl)-7H-pyrrolo[2,3-d]pyrimidin-4-amine **(13).** Yellow powder, yield 31%, mp: 333 °C. ^{1}H NMR (600 MHz, DMSO-d_6) δ 11.97 (br s, 1H, NH, H-7), 9.99 (s, 1H, N–H), 8.43 (s, 1H, H-2), 8.27–821 (m, 4H, Ar–H), 7.36 (d, $J = 3.5$ Hz, 1H, H-6), 6.89 (d, $J = 3.5$ Hz, 1H, H-5). ^{13}C NMR (151 MHz, DMSO-d_6) δ 152.4, 151.4, 150.3, 147.2, 140.6, 124.8, 123.4, 118.6, 104.7, 98.6. HRMS (APCI) *m/z* $[M+H]^+$ calcd for $C_{12}H_{10}N_5O_2$ $[M+H]^+$: 256.0829, found: 256.0817.

N-(2-methoxy-4-nitrophenyl)-7H-pyrrolo[2,3-d]pyrimidin-4-amine **(14).** White powder, yield 50%, mp: 310 °C. ^{1}H NMR (600 MHz, DMSO-d_6) δ 11.96 (br s, 1H, NH, H-7), 8.75 (s, 1H, NH), 8.67 (d, $J = 9.0$ Hz, 1H, Ar–H), 8.38 (s, 1H, H-2), 7.96 (dd, $J = 8.9$, 2.5 Hz, 1H, Ar–H), 7.85 (d, $J = 2.6$ Hz, 1H, Ar–H), 7.35 (d, $J = 3.5$ Hz, 1H, H-6), 6.87 (d, $J = 3.5$ Hz, 1H, H-5), 4.03 (s, 3H, CH_3). ^{13}C NMR (151 MHz, DMSO-d_6) δ 152.4, 151.5, 150.4, 148.8, 141.5, 135.7, 123.6, 119.8, 117.0, 105.8, 104.7, 98.5, 56.5. HRMS (APCI) *m/z*: calcd for $C_{13}H_{12}N_5O_3$ $[M+H]^+$: 286.0935, found: 286.0920.

N-(4-morpholinophenyl)-7H-pyrrolo[2,3-d]pyrimidin-4-amine **(15).** Grey powder, yield 27%, mp > 400 °C. ^{1}H NMR (600 MHz, DMSO-d_6) δ 11.50 (br s, 1H, NH, H-7), 8.97 (s, 1H, NH), 8.19 (s, 1H, H-2), 7.65 (d, $J = 6.7$ Hz, 2H, Ar–H), 7.13 (d, $J = 3.4$ Hz, 1H, H-6), 6.93 (d, $J = 9.0$ Hz, 2H, Ar–H), 6.63 (d, $J = 3.5$ Hz, 1H, H-5), 3.85–3.64 (m, 4H, 2X CH_2), 3.14–2.96 (m, 4H, 2X CH_2). ^{13}C NMR (151 MHz, DMSO-d_6) δ 153.8, 150.7, 150.6, 146.7, 132.4, 122.0, 121.3, 115.3, 103.0, 98.6, 65.9, 49.0. HRMS (APCI) *m/z*: calcd for $C_{16}H_{18}N_5O$ $M+H]^+$: 296.1506, found: 296.1481.

N-benzyl-7H-pyrrolo[2,3-d]pyrimidin-4-amine **(16).** White powder, yield 34%, mp 207 °C. ^{1}H NMR (600 MHz, DMSO-d_6) δ 11.46 (s, 1H), 8.09 (s, 1H), 7.87 (t, $J = 6.1$ Hz, 1H), 7.35 (d, $J = 7.1$ Hz, 2H), 7.30 (t, $J = 7.6$ Hz, 2H), 7.22 (t, $J = 7.3$ Hz, 1H), 7.07 (dd, $J = 3.5$, 2.0 Hz, 1H), 6.58 (dd, $J = 3.5$, 1.5 Hz, 1H). ^{13}C NMR (151 MHz, DMSO-d_6) δ 155.9, 151.3, 150.2, 140.4, 128.1, 127.1, 126.5, 120.8, 102.5, 98.5, 43.1. HRMS (APCI) *m/z* $[M+H]^+$ calcd for $C_{13}H_{12}N_4$ $[M+H]^+$: 225.1135, found 225.1151.

N-(pyridin-3-ylmethyl)-7H-pyrrolo[2,3-d]pyrimidin-4-amine **(17).** Yellow powder, yield 34%, mp 260 °C ^{1}H NMR (600 MHz, DMSO-d_6) δ 11.54 (brs, 1H, NH, H-7), 8.58 (d, $J = 2.1$ Hz, 1H, pyridyl), 8.44 (dd, $J = 4.8$, 1.6 Hz, 1H, pyridyl), 8.11 (s, 1H, H-2), 7.98 (t, $J = 6.1$ Hz, 1H, NH), 7.74 (dt, $J = 7.9$, 2.0 Hz, 1H, pyridyl), 7.33 (dd, $J = 7.8$, 4.7 Hz, 1H, pyridyl), 7.09 (dd, $J = 3.4$, 2.2 Hz, 1H, H-6), 6.56 (dd, $J = 3.5$, 1.7 Hz, 1H, H-5), 4.72 (d, $J = 5.9$ Hz, 2H, CH_2). ^{13}C NMR (151 MHz, DMSO-d_6) δ 155.8, 151.3, 150.2, 148.9, 147.9, 135.8, 135.1, 123.4, 121.1, 102.6, 98.5.

HRMS (ESI+) *m/z* $[M+H]^+$ calcd for $C_{12}H_{12}N_5$ $[M+H]^+$: 226.1101, found: 226.1091.

N-(pyridin-2-ylmethyl)-7H-pyrrolo[2,3-d]pyrimidin-4-amine **(18).** Yellow powder, yield 48%, mp 181 °C. ^{1}H NMR (600 MHz, DMSO-d_6) δ 11.50 (brs, 1H, NH), 8.51 (d, J = 4.8 Hz, 1H, pyridyl), 8.08 (s, 1H, pyridyl, 7.98 (t, J = 6.2 Hz, 1H, 1H, NH),), 7.70 (td, J = 7.7, 1.8 Hz, 1H, pyridy), 7.32 (d, J = 7.9 Hz, 1H, pyridyl), 7.23 (ddd, J = 7.5, 4.8, 1.2 Hz, 1H), 7.09 (dd, J = 3.4, 2.0 Hz, 1H, H-6), 6.61 (dd, J = 3.5, 1.6 Hz, 1H, H-5), 4.80 (d, J = 6.1 Hz, 2H, CH_2). ^{13}C NMR (151 MHz,) δ 159.6, 155.9, 151.3, 150.2, 148.7, 136.5, 121.8, 120.9, 120.9, 102.6, 98.5, 45.2. HRMS (APCI) *m/z*: calcd for $C_{12}H_{12}N_5$ $[M+H]^+$: 226.1087, found 226.1088.

N-(4-methylbenzyl)-7H-pyrrolo[2,3-d]pyrimidin-4-amine **(19).** Brown powder, yield 34%, mp 200 °C. ^{1}H NMR (600 MHz, DMSO-d_6) δ 11.48 (br s, 1H), 8.08 (s, 1H, H-2), 7.87 (t, J = 6.0 Hz, 1H. NH), 7.30–7.17 (m, 2H, Ar–H), 7.11 (d, J = 7.9 Hz, 2H, Ar–H),), 7.06 (dd, J = 3.4, 2.2 Hz, 1H, Ar–H),), 6.57 (dd, J = 3.4, 1.8 Hz, 1H, Ar–H),), 4.66 (d, J = 6.0 Hz, 2H, CH_2), 2.26 (s, 3H, CH_2). ^{13}C NMR (151 MHz, DMSO-d_6) δ 155.9, 151.4, 150.2, 137.3, 135.6, 128.8, 127.2, 120.8, 102.5, 98.6, 42.9, 20.7. HRMS (APCI) *m/z*: calcd for $C_{14}H_{15}N_4$ $[M+H]^+$: 239.1291, found: 239.1310.

*N-(4-chlorobenzyl)-7H-pyrrolo[2,3-d]pyrimidin-4-*amine **(20).** Yellow powder, yield 59%, mp 199 °C ^{1}H NMR (600 MHz, DMSO-d_6) δ 11.54 (br s, 1H, NH, 7-H), 8.09 (s, 1H, H-2), 7.98 (t, J = 6.1 Hz, 1H, NH), 7.38 (s, 1H, Ar–H), 7.38–7.27 (m, 3H, Ar–H), 7.10 (dd, J = 3.4, 2.2 Hz, 1H, H-6), 6.57 (dd, J = 3.5, 1.8 Hz, 1H, H-5), 4.71 (d, J = 6.1 Hz, 2H, CH_2). ^{13}C NMR (151 MHz, DMSO-d_6) δ 155.9, 151.4, 150.2, 143.2, 132.9, 130.2, 126.9, 126.6, 125.9, 121.1, 102.6, 98.5, 42.3. HRMS (APCI) *m/z*: calcd for $C_{13}H_{12}ClN_4$ $[M+H]^+$: 259.0745, found: 259.0735.

N-phenylethyl-7H-pyrrolo[2,3-d]pyrimidin-4-amine **(21).** White powder, yield 58%, mp 195 °C. ^{1}H NMR (600 MHz, DMSO-d_6) δ 11.46 (br s, 1H, NH), 8.11 (s, 1H, H-2), 7.48 (t, J = 5.7 Hz 1H, NH), 7.32–7.23 (m, 4H, Ar–H), 7.21–7.16 (m, 1H, Ar–H), 7.04 (dd, J = 3.4, 2.1 Hz, 1H, H-6), 6.52 (dd, J = 3.4, 1.7 Hz, 1H, H-5), 3.70–3.63 (m, 2H, CH_2), 2.93–2.87 (m, 2H, CH_2). ^{13}C NMR (151 MHz, DMSO-d_6) δ 156.0, 151.5, 150.1, 139.8, 128.7, 128.3, 126.0, 120.7, 102.6, 98.5, 41.7, 35.4. HRMS (APCI) *m/z*: calcd for $C_{14}H_{15}N_4$ $[M+H]^+$: 239.1291, found: 239.1283.

N-(3-phenylpropyl)-7H-pyrrolo[2,3-d]pyrimidin-4-amine **(22).** White powder, yield 37%, mp 144 °C. ^{1}H NMR (600 MHz, DMSO-d_6) δ 11.42 (br s, 1H, NH, H-7), 8.06 (s, 1H, H-2), 7.41 (t, J = 5.6 Hz, 1H, NH), 7.27 (t, J = 7.5 Hz, 2H, Ar–H), 7.23–7.20 (m, 2H, Ar–H), 7.16 (t, J = 7.2 Hz, 1H, Ar–H), 7.04 (d, J = 3.4 Hz, 1H, H-6), 6.53 (d, J = 3.4 Hz, 1H, H-5), 3.47–3.43 (m, 2H, CH_2), 2.65 (t, J = 7.7 Hz, 2H, CH_2), 1.89 (m, 2H, CH_2).^{13}C NMR (151 MHz, DMSO-d_6) δ 156.3, 151.6, 150.1, 142.0, 128.8, 128.5 125.9, 120.9, 102.6, 98.8, 39.2, 32.9, 31.2. HRMS (APCI) *m/z*: calcd for $C_{15}H_{17}N_4$ $[M+H]^+$: 253.1448, found: 253.1453.

N-(4-phenylbutyl)-7H-pyrrolo[2,3-d]pyrimidin-4-amine **(23).** Yellow powder, yield 49%, mp 128 °C. ^{1}H NMR (600 MHz, DMSO-d_6) δ 11.43 (br s, 1H, NH, H-7), 8.07 (s, 1H, H-2), 7.35 (t, J = 5.7 Hz, 1H, N–H), 7.25 (t, J = 7.6 Hz, 2H, Ar–H),), 7.19 (d, J = 6.8 Hz, 2H, Ar–H),), 7.15 (t, J = 7.3 Hz, 1H, Ar–H),), 7.03 (d, J = 3.4 Hz, 1H, H-6), 6.52 (d, J = 3.4 Hz, 1H, H-5), 3.47 (q, J = 6.5 Hz, 2H), 2.61 (t, J = 7.3 Hz, 2H), 1.67–1.57 (m, 4H). ^{13}C NMR (151 MHz, DMSO-d_6) δ 156.2, 151.5, 150.0, 142.2, 128.4, 128.3, 125.7, 120.6, 102.5, 98.6, 39.2, 34.9, 29.0, 28.6. HRMS (APCI) *m/z*: calcd for $C_{16}H_{19}N_4$ $[M+H]^+$: 267.1604, found 267.1619.

N-(3-chlorophenethyl)-7H-pyrrolo[2,3-d]pyrimidin-4-amine **(24).** Grey powder, yield 66%, 163 °C. ^{1}H NMR (600 MHz, DMSO-d_6) δ 11.46 (br s, 1H, H-7), 8.11 (s, 1H, H-2), 7.48 (t, 5.9 Hz, 1H, NH), 7.34–7.33 (m, 1H, Ar–H), 7.31 (d, J = 7.7 Hz, 1H, Ar–H), 7.25 (d, J = 9.0 Hz, 1H, Ar–H), 7.22 (d, J = 7.5 Hz, 1H, Ar–H), 7.05 (dd, J = 3.4, 2.3 Hz, 1H, H-6),, 6.51 (dd, J = 3.4, 1.9 Hz, 1H), 3.68 (q, J = 6.9 Hz, 2H), 2.93 (t, J = 7.3 Hz, 2H).^{13}C NMR (151 MHz, DMSO-d_6) δ 155.9, 151.4, 150.0, 148.6, 142.5, 132.9, 130.1, 128.5, 127.5, 126.0, 120.7, 98.5, 48.6, 34.8. HRMS (APCI) *m/z*: calcd for $C_{16}H_{19}N_4$ $[M+H]^+$: 273.0902, found 273.0917.

N-isopentyl-7H-pyrrolo[2,3-d]pyrimidin-4-amine **(25).** Brown powder, yield 64%, mp 159 °C. ^{1}H NMR (600 MHz, DMSO-d_6) δ 11.42 (br s, 1H, NH, H-7), 8.07 (s, 1H, H-2), 7.28 (t, J = 5.6 Hz, 1H, NH), 7.03 (dd, J = 3.4, 2.0 Hz, 1H, H-6), 6.52 (dd, J = 3.3, 1.6 Hz, 1H, H-5), 3.50–3.44 (m, 2H, CH_2), 1.70–1.61 (m, J = 6.7 Hz, 1H, CH), 1.48 (q, J = 7.0 Hz, 2H, CH_2), 0.92 (s, 3H, CH_3), 0.90 (s, 3H, CH_3). ^{13}C NMR (151 MHz, DMSO-d_6) δ 156.2, 151.5, 150.0, 120.6, 102.5, 98.6, 38.3, 38.2, 25.4, 22.6. HRMS (APCI) *m/z* $[M+H]^+$ calcd for $C_{11}H_{17}N_4[M+H]^+$: 205.1448, found 205.1452.

2-((2-((7H-pyrrolo[2,3-d]pyrimidin-4-yl)amino)ethyl) amino)ethan-1-ol **(26).** White powder, yield 52,5%, mp 161 °C. ^{1}H NMR (600 MHz, DMSO-d_6) δ 11.46 (br s, 1H, NH, H-7), 8.09 (s, 1H, H-2),), 7.35 (t, J = 5.6 Hz, 1H, NH), 7.05 (d, J = 3.4 Hz, 1H, H-6), 6.54 (d, J = 3.4 Hz, 1H, H-5), 3.54 (q, J = 6.3 Hz, 2H, CH_2), 3.46 (t, J = 5.7 Hz, 2H, CH_2), 3.18 (br s, 1H, OH), 2.77 (t, J = 6.5 Hz, 2H, CH_2), 2.63 (t, J = 5.7 Hz, 2H, CH_2). ^{13}C NMR (151 MHz, DMSO-d_6) δ 156.2, 151.4, 150.1, 120.6, 102.5, 98.6, 60.4, 60.2, 51.6, 48.8. HRMS (APCI) *m/z*: calcd for $C_{10}H_{16}N_5O$ $[M+H]^+$: 222.1349, found: 222.1368.

N-(3-isopropoxypropyl)-7H-pyrrolo[2,3-d]pyrimidin-4-amine **(27).** Brown powder, yield 25%, mp 129 °C. ^{1}H NMR (600 MHz, DMSO-d_6) δ 11.43 (brs, 1H, NH), 8.07 (s, 1H, H-2), 7.35 (t, J = 5.7 Hz,1H, NH), 7.04 (dd, J = 3.4,

2.0 Hz, 1H, H-6), 6.51 (dd, $J = 3.4$, 1.6 Hz, 1H, H-5), 3.53–3.47 (m, 3H, OCH_2 and CH), 3.44 (t, $J = 6.3$ Hz, 2H, CH_2), 1.79 (m, 2H, CH_2), 1.08 (d, $J = 6.1$ Hz, 6H, $2 \times CH_3$). ^{13}C NMR (151 MHz, DMSO-d_6) δ 156.2, 151.5, 150.0, 120.6, 102.5, 98.5, 70.60, 65.3, 37.4, 29.9, 22.1. HRMS (APCI) *m/z*: calcd for $C_{12}H_{19}N_4O$ $[M + H]^+$: 235.1553, found: 235.1546.

N-(3-morpholinopropyl)-7H-pyrrolo[2,3-d]pyrimidin-4-amine **(28).** Brown powder, yield 16%, mp: 170 °C. ^1H NMR (600 MHz, DMSO-d_6) δ 11.44 (br s, 1H, NH, 7-H), 8.07 (s, 1H, H-2), 7.36 (t, $J = 5.6$ Hz,1H), 7.04 (d, $J = 3.4$ Hz, 1H, H-6), 6.51 (d, $J = 3.4$ Hz, 1H, H-5), 3.57 (t, $J = 4.7$ Hz, 4H, 2 X CH_2), 3.50–3.44 (m, 2H, CH_2), 2.37–2.34 (m, 6H, 3X CH_2), 1.75 (m, 2H, CH_2). ^{13}C NMR (151 MHz, DMSO-d_6) δ 156.1, 151.5, 150.0, 120.6, 102.5, 98.5, 66.2, 56.2, 53.4, 48.6, 26.1. HRMS (APCI) *m/z* $[M + H]^+$ calcd for $C_{13}H_{20}N_5O$ $[M + H]^+$: 261.1662, found: 262.1675.

4-(7H-pyrrolo[2,3-d]pyrimidin-4-yl)morpholine **(29).** Brown powder, yield 94%, mp 207 °C. ^1H NMR (600 MHz, DMSO-d_6) ^1H NMR (600 MHz, DMSO-d_6) δ 11.72 (br s, 1H, NH, H-7), 8.16 (s, 1H, H-2), 7.20 (dd, $J = 3.6$, 2.3 Hz, 1H, H-6), 6.62 (dd, $J = 3.7$, 1.7 Hz, 1H, H-5), 3.88–3.80 (m, 4H, 2X OCH_2), 3.74–3.67 (m, 4H, 2X CH_2). ^{13}C NMR (151 MHz, DMSO-d_6) δ 156.6, 152.0, 150.4, 121.6, 102.3, 100.8, 66.1, 45.5. HRMS (APCI) *m/z*: calcd for $C_{10}H_{13}N_4O$ $[M + H]^+$: 205.1084, found: 205.1099.

N-(cyclohexylmethyl)-7H-pyrrolo[2,3-d]pyrimidin-4-amine **(30).** White powder, yield 87%, mp 179 °C. ^1H NMR (600 MHz, DMSO-d_6) δ 11.41 (br s, 1H, NH), 8.06 (s, 1H, H-2), 7.33 (t, $J = 5.6$ Hz, 1H, NH), 7.02 (d, $J = 3.4$ Hz, 1H, H-6), 6.55 (s, 1H, H-5), 3.29 (t, $J = 6.4$ Hz, 2H, CH_2), 1.71 (m, 4H, $2 \times CH_2$), 1.63–1.58 (m, 2H, CH_2), 1.63–1.58 (m, 2H CH_2), 1.16 (q, $J = 12.8$ Hz, 3H, CH and CH_2), 0.93 (q, $J = 11.9$ Hz, 2H, CH_2). ^{13}C NMR (151 MHz, DMSO-d_6) δ 156.3, 151.4, 150.0, 120.5, 102.4, 98.6, 46.2, 37.4, 30.6, 26.2, 25.5. HRMS (APCI) *m/z*: calcd for $C_{13}H_{19}N_4$ $[M + H]^+$: 231.1604, found: 231.1618.

N-cyclopentyl-7H-pyrrolo[2,3-d]pyrimidin-4-amine **(31).** Brown powder, yield 46%, mp 157 °C ^1H NMR (600 MHz, DMSO-d_6) δ 11.28 (br s, 1H, NH, H-7), 8.08 (s, 1H, H-2), 7.02 (d, $J = 3.4$ Hz, 1H, H-6), 6.58 (d, $J = 3.4$ Hz, 1H, H-5), 4.51–4.55 (m, 1H), 2.01–1.95 (m, 2H, CH_2), 1.72 (d, $J = 3.8$ Hz, 2H, CH_2), 1.60–1.51 (m, 4H, 2X CH_2). ^{13}C NMR (151 MHz, DMSO-d_6) δ 155.7, 151.2, 150.0, 120.2, 102.3, 98.6, 51.4, 32.3, 23.4. HRMS (APCI) *m/z*: calcd for $C_{11}H_{15}N_4$ $[M + H]^+$: 203,1291, found: 203.1287.

Biological evaluation

In vitro antimycobacterial assay

In vitro antitubercular activity was evaluated essentially as described by Dube et al. (2021) [42]. A 10 mL culture of the test organism, *Mtb* pMSp12: GFP, was grown on a Middlebrook 7H9 enriched with 0.03% casitone, 0.4% glucose, and 0.05% tyloxapol, to an optical density (0D600) of 0.6–0.7. The different concentration of the test compounds was made up to 10 mM in DMSO, from which twofold serial dilutions were made and transferred to 96-well plates, and 50 mL of the diluted *Mtb* culture was then added to each well. Rifampicin and 5% DMSO were used as a minimum growth control and maximum growth control, respectively. The microtitre plates were sealed and incubated at 37 °C with 5% CO_2 and humidification. On day 14, fluorescence readings were determined at excitation 485 nM; emission 520 nM using A SpecraMax i3x Plate reader: (Serial no. 36370 3271), Molecular Devices Corporation 1311 Orleans Drive Sunnyvale, California 94,089. The Softmax ® Pro 6, 4-parameter curve fit protocol is used to generate a calculated MIC_{90}. To generate a dose–response curve (% inhibition), the raw data were normalized to the minimum and maximum inhibition controls using the Levenberg–Marquardt damped least-squares method, from which the minimum inhibitory concentration (MIC) MIC_{90} is calculated. The concentration at which growth inhibition was higher than 90% was taken as the MIC_{90}.

Evaluation of cytotoxic activity

Cells were seeded at different densities, specifically, BJ-5ta at 1.8×10^4 cells/well and Vero at 3.0×10^3 cells/well and incubated for 24 h in 5% CO_2 at 37 °C. Adherent cells were exposed to three concentrations (1, 5, and 10 µM) of the test compound BO126 (Mw 302.33 g/mol) dissolved in 0.15% DMSO and incubated for another 48 h. The compound was tested with 3 technical repeats, and 0.2% Triton X-100 (TX-100), known to induce cell-apoptosis [43], was used as an experimental positive control (dead cell control). Thereafter, spent media and treatment were aspirated, and cells were rinsed twice with 100 µl PBS. This was followed by the addition of 200 µl MTT solution at a final concentration of 0.5 mg/ml to each well according to the standard operation procedure and incubated for 4 h. To measure the effect of TX-100, at the end of the experiment, untreated cells were rinsed following the same method as other experimental groups and exposed to TX-100 for 15 min before the addition of MTT solution. At the end of the incubation period, MTT solution was removed and 200 µl of DMSO was added to solubilize the formed formazan crystals. Plates were then shaken for additional 15 min after a 1 h incubation, and absorbances were determined at 560 nm against the background signal at 630 nm.

Cell survival rate expressed relative to untreated cell control was calculated according to the following equation:

$$\text{Cell survival (\%)} = \frac{\Delta\text{Test sample} - \Delta\text{Blank}}{\Delta\text{Control} - \Delta\text{Blank}} \times 100$$

where Δ Test sample = Test sample absorbance at 560 nm –Test sample absorbance at 630 nm.

Δ Blank = DMSO blank at 560 nm–DMSO blank 630 nm.

Δ Control = Untreated cells at 560 nm–Untreated cells at 630 nm.

Supplementary Information The online version contains supplementary material available at https://doi.org/10.1007/s11030-022-10453-1.

Acknowledgements This work was supported by North-West University, Postdoctoral Funding and DSI/NRF Innovation Postdoctoral Fellowship (Grant no: 129647) awarded to O.J. Jesumoroti. The authors appreciate financial and infrastructural support from North-West University, Potchefstroom campus. We are grateful to Dr. Otto Daniel and Dr. Johan Jordaan of the SASOL Centre for Chemistry, North-West University for the generation of NMR and HRMS data, respectively.

Data availability & Supplementary Biological data that support the findings of this study are openly available in manuscripts, figures, and tables. IH NMR 13C NMR, IR, HRMS spectra of all these synthesized compounds are provided in supplementary.

Declarations

Conflict of Interest The authors declare that there is no conflict of interest.

Ethics Approval Ethics approval was obtained from North-West University Health Research Ethics Committee (NWU-HREC) ON 12/10/2020. NWU-00471–20-A1 Potchefstroom, South Africa.

References

1. Aher RB, Sarkar D (2021) 2D-QSAR modeling and two-fold classification of 1, 2, 4-triazole derivatives for antitubercular potency against the dormant stage of Mycobacterium tuberculosis. Mol Divers 24:1–16. https://doi.org/10.1007/s11030-021-10254-y
2. World Health Organization (2020) Global TB Rep 2020:9789241565714
3. World Health Organization (2021) Global Tuberculosis Report 2021.
4. Chakaya J, Khan M, Ntoumi F, Aklillu E, Fatima R, Mwaba P, Kapata N, Mfinanga S, Hasnain SE, Katoto PD (2021) Global Tuberculosis Report 2020–Reflections on the Global TB burden, treatment and prevention efforts. Int J Infect Dis. https://doi.org/10.1016/j.ijid.2021.02.107
5. Satish S, Chitral R, Kori A, Sharma B, Puttur J, Khan AA, Desle D, Raikuvar K, Korkegian A, Martis EA (2021) Design, synthesis and SAR of antitubercular benzylpiperazine ureas. Mol Divers 26:1–24. https://doi.org/10.1007/s11030-020-10158-3
6. Parker WB, Long MC (2007) Purine metabolism in Mycobacterium tuberculosis as a target for drug development. Curr Pharm Des 13:599–608. https://doi.org/10.2174/138161207780162863
7. Villemagne B, Crauste C, Flipo M, Baulard AR, Déprez B, Willand N (2012) Tuberculosis: the drug development pipeline at a glance. Eur J Med Chem 51:1–16. https://doi.org/10.1016/j.ejmech.2012.02.033
8. Dasari R, Kornienko A (2014) Multicomponent synthesis of the medicinally important pyrrolo [2, 3-d] pyrimidine scaffold (minireview). Chem Heterocycl Compd (N Y) 50:139–144. https://doi.org/10.1007/s10593-014-1456-9
9. Sabat N, Poštová Slavětínská L, Klepetářová B, Hocek M (2018) C-H Imidation of 7-Deazapurines. ACS Omega 3:4674–4678. https://doi.org/10.1021/acsomega.8b00520
10. Pathania S, Rawal RK (2018) Pyrrolopyrimidines: an update on recent advancements in their medicinal attributes. Eur J Med Chem 157:503–526. https://doi.org/10.1016/j.ejmech.2018.08.023
11. van der Westhuyzen AE, Frolova LV, Kornienko A, van Otterlo WA (2018) Biology. The Rigidins: Isolation, Bioactivity, and Total Synthesis—Novel Pyrrolo [2, 3-d] Pyrimidine Analogues Using Multicomponent Reactions. In: Knölker H-J (ed) The alkaloids: chemistry. Academic Press: 2018; Volume 79, pp. 191–220.
12. Bhat KI, Kumar A, Nisar M, Kumar P (2014) Synthesis, pharmacological and biological screening of some novel pyrimidine derivatives. Med Chem Res 23:3458–3467. https://doi.org/10.1007/s00044-014-0914-3
13. Patil SB (2018) Biological and medicinal significance of pyrimidines:a review. Int J Pharm Sci Res 9:44–52
14. Kumar S, Narasimhan B (2018) Therapeutic potential of heterocyclic pyrimidine scaffolds. Chem Cent J 12:38. https://doi.org/10.1186/s13065-018-0406-5
15. Vazirimehr S, Davoodnia A, Beyramabadi SA, Nakhaei-Moghaddam M, Tavakoli-Hoseini N (2017) Two new pyrrolo[2,3-d]pyrimidines (7-deazapurines): ultrasonic-assisted synthesis, experimental and theoretical characterizations as well as antibacterial evaluation Z Naturforsch B 72:481–487. https://doi.org/10.1515/znb-2017-0004.
16. Hilmy KMH, Khalifa MM, Hawata MAA, Keshk RMA (2010) Synthesis of new pyrrolo [2, 3-d] pyrimidine derivatives as antibacterial and antifungal agents. Eur J Med Chem 45:5243–5250. https://doi.org/10.1016/j.ejmech.2010.08.043
17. Hess S, Müller CE, Frobenius W, Reith U, Klotz K-N, Eger K (2000) 7-Deazaadenines bearing polar substituents: structure—activity relationships of New A1 and A3 Adenosine receptor antagonists. J Med Chem 43:4636–4646. https://doi.org/10.1021/jm000967d
18. Caldwell JJ, Davies TG, Donald A, McHardy T, Rowlands MG, Aherne GW, Hunter LK, Taylor K, Ruddle R, Raynaud FI (2008) Identification of 4-(4-aminopiperidin-1-yl)-7 H-pyrrolo [2, 3-d] pyrimidines as selective inhibitors of protein kinase B through fragment elaboration. J Med Chem 51:2147–2157. https://doi.org/10.1021/jm701437d
19. Mohamed MS, Kamel R, Fatahala SS (2010) Synthesis and biological evaluation of some thio containing pyrrolo [2, 3-d] pyrimidine derivatives for their anti-inflammatory and anti-microbial activities. Eur J Med Chem 45:2994–3004. https://doi.org/10.1016/j.ejmech.2010.03.028
20. Zhang J, Chen P, Duan Y, Xiong H, Li H, Zeng Y, Liang G, Tang Q, Wu D (2021) Design, synthesis and biological evaluation of 7H-pyrrolo [2, 3-d] pyrimidine derivatives containing 1, 8-naphthyridine-4-one fragment. Eur J Med Chem 215:113273. https://doi.org/10.1016/j.ejmech.2021.113273
21. Günther M, Laux J, Laufer S (2019) Synthesis and structure-activity-relationship of 3, 4-Diaryl-1H-pyrrolo [2, 3-b] pyridines as irreversible Inhibitors of mutant EGFR-L858R/T790M. Eur J Pharm Sci 128:91–96. https://doi.org/10.1016/j.ejmech.2017.12.079
22. Gangjee A, Zeng Y, McGuire JJ, Mehraein F, Kisliuk RL (2004) Synthesis of classical, three-carbon-bridged 5-substituted furo [2, 3-d] pyrimidine and 6-substituted pyrrolo [2, 3-d] pyrimidine analogues as antifolates. J Med Chem 47:6893–6901. https://doi.org/10.1021/jm040123k

23. Liang X, Tang S, Liu X, Liu Y, Xu Q, Wang X, Saidahmatov A, Li C, Wang J, Zhou Y (2021) Discovery of Novel Pyrrolo [2, 3-d] pyrimidine-based derivatives as potent JAK/HDAC dual inhibitors for the treatment of refractory solid tumors. J Med Chem. https://doi.org/10.1021/acs.jmedchem.0c02111
24. Perlíková P, Hocek M (2017) Pyrrolo [2, 3-d] pyrimidine (7-deazapurine) as a privileged scaffold in design of antitumor and antiviral nucleosides. Med Res Rev 37:1429–1460. https://doi.org/10.1002/med.21465
25. Perlíková P, Konečný P, Nauš P, Snášel J, Votruba I, Džubák P, Pichová I, Hajdúch M, Hocek M (2013) 6-Alkyl-, 6-aryl-or 6-hetaryl-7-deazapurine ribonucleosides as inhibitors of human or MTB adenosine kinase and potential antimycobacterial agents. MedChemComm 4:1497–1500. https://doi.org/10.1039/C3MD00232B
26. Malnuit V, Slavětínská LP, Nauš P, Džubák P, Hajdúch M, Stolaříková J, Snášel J, Pichová I, Hocek M (2015) 2-Substituted 6-(Het) aryl-7-deazapurine ribonucleosides: synthesis, inhibition of adenosine kinases, and antimycobacterial activity. ChemMedChem 10:1079–1093. https://doi.org/10.1002/cmdc.201500081
27. Naus P, Caletkova O, Konecny P, Dzubak P, Bogdanova K, Kolar M, Vrbkova J, Slavetinska L, Tloušťová E, Perlikova P (2014) Synthesis, cytostatic, antimicrobial, and anti-HCV activity of 6-substituted 7-(het) aryl-7-deazapurine ribonucleosides. J Med Chem 57:1097–1110. https://doi.org/10.1021/jm4018948
28. Anzai K, Nakamura G, Suzuki S (1957) A new antibiotic, tubercidin. J Antibiot Series A 10:201–204. https://doi.org/10.11554/antibioticsa.10.5_201.
29. Matsuoka M, Umezawa H (1960) Unamycin, an antifungal substance produced by Streptomyces fungicidicus. J Antibiot Series A 13:114–120. https://doi.org/10.11554/antibioticsa.13.2_114.
30. De Clercq E, Balzarini J, Madej D, Hansske F, Robins MJ (1987) Nucleic acid related compounds. 51. Synthesis and biological properties of sugar-modified analogs of the nucleoside antibiotics tubercidin, toyocamycin, sangivamycin, and formycin. J Med Chem 30:481–486. https://doi.org/10.1021/jm00386a007
31. Ding Y, An H, Hong Z, Girardet J-L (2005) Synthesis of 2′-β-C-methyl toyocamycin and sangivamycin analogues as potential HCV inhibitors. Bioorg Med Chem Lett 15:725–727. https://doi.org/10.1016/j.bmcl.2004.11.019
32. Raju KS, AnkiReddy S, Sabitha G, Krishna VS, Sriram D, Reddy KB, Sagurthi SR (2019) Synthesis and biological evaluation of 1H-pyrrolo [2, 3-d] pyrimidine-1, 2, 3-triazole derivatives as novel anti-tubercular agents. Bioorg Med Chem Lett 29:284–290. https://doi.org/10.1016/j.bmcl.2018.11.036
33. Khoje AD, Kulendrn A, Charnock C, Wan B, Franzblau S, Gundersen L-L (2010) Synthesis of non-purine analogs of 6-aryl-9-benzylpurines, and their antimycobacterial activities. Compounds modified in the imidazole ring. Bioorg Med Chem Lett 18:7274–7282. https://doi.org/10.1016/j.bmc.2010.08.016
34. Kurup S, McAllister B, Liskova P, Mistry T, Fanizza A, Stanford D, Slawska J, Keller U, Hoellein A (2018) Design, synthesis and biological activity of N 4-phenylsubstituted-7 H-pyrrolo [2, 3-d] pyrimidin-4-amines as dual inhibitors of aurora kinase A and epidermal growth factor receptor kinase. J Enzyme Inhib Med Chem 33:74–84. https://doi.org/10.1080/14756366.2017.1376666
35. Katritzky A (2012) Physical methods in heterocyclic chemistry V3, vol 3. Elsevier: New York.
36. López-García J, Lehocký M, Humpolíček P, Sáha P (2014) HaCaT keratinocytes response on antimicrobial atelocollagen substrates: extent of cytotoxicity, cell viability and proliferation. J Funct Biomater 5:43–57. https://doi.org/10.3390/jfb5020043
37. O'Shea R, Moser HE (2008) Physicochemical properties of antibacterial compounds: implications for drug discovery. J Med Chem 51:2871–2878. https://doi.org/10.1021/jm700967e
38. Delaney JS (2004) ESOL: estimating aqueous solubility directly from molecular structure. J Chem Inf Comput Sci 44:1000–1005. https://doi.org/10.1021/ci034243x
39. Ali J, Camilleri P, Brown MB, Hutt AJ, Kirton SB (2012) Revisiting the general solubility equation: in silico prediction of aqueous solubility incorporating the effect of topographical polar surface area. J Chem Inf Model 52:420–428. https://doi.org/10.1021/ci200387c
40. Veber DF, Johnson SR, Cheng H-Y, Smith BR, Ward KW, Kopple KD (2002) Molecular properties that influence the oral bioavailability of drug candidates. J Med Chem 45:2615–2623. https://doi.org/10.1021/jm020017n
41. Lipinski CA, Lombardo F, Dominy BW, Feeney PJ (1997) Experimental and computational approaches to estimate solubility and permeability in drug discovery and development settings. Adv Drug Deliv Rev 23:3–25. https://doi.org/10.1016/S0169-409X(96)00423-1
42. Dube PS, Legoabe LJ, Jordaan A, Jesumoroti OJ, Tshiwawa T, Warner DF, Beteck RM (2021) Easily accessed nitroquinolones exhibiting potent and selective anti-tubercular activity. Eur J Med Chem 213:113207. https://doi.org/10.1016/j.ejmech.2021.113207
43. Ahn JM, Kim SJ, Kim H, Park C, Kim WH, Park JH (1997) Triton X-100 induces apoptosis in human hepatoma cell lines. Yonsei Med J 38:52–59. https://doi.org/10.3349/ymj.1997.38.1.52

Authors and Affiliations

Omobolanle Janet Jesumoroti[1] · Richard M. Beteck[1] · Audrey Jordaan[2] · Digby F. Warner[2,3,4] · Lesetja J. Legoabe[1]

[1] Centre of Excellence for Pharmaceutical Sciences, North-West University, Private Bag X6001, Potchefstroom 2520, South Africa

[2] SAMRC/NHLS/UCT Molecular Mycobacteriology Research Unit, Department of Pathology, University of Cape Town, Observatory 7925, South Africa

[3] Institute of Infectious Disease and Molecular Medicine, University of Cape Town, Rondebosch 7701, South Africa

[4] Wellcome Centre for Infectious Diseases Research in Africa (CIDRI-Africa), Faculty of Health Sciences, University of Cape Town, Rondebosch 7701, South Africa